Electronic structure of CrN: A borderline Mott insulator

Aditi Herwadkar* and Walter R. L. Lambrecht
Department of Physics, Case Western Reserve University, Cleveland, Ohio 44106-7079, USA
(Received 23 June 2008; published 29 January 2009)

Calculations using the LSDA+U (local spin-density approximation corrected by Hubbard Coulomb terms for the *d* electrons) approach show that CrN is close to a charge-transfer insulator transition. The values of *U* are estimated in various ways, including the recently developed linear-response approach. With reasonable values of *U* in the range of 3–5 eV it is found that the density of states near the Fermi level is strongly depleted by the spin separation of the states. In the case of the antiferromagnetic (AFM)-$[110]_2$ configuration a small gap actually opens even for *U* as small as 3 eV. Furthermore a smallest direct gap of about 1 eV can be seen in these band structures and could be responsible for the onset of strong optical absorption observed to occur at 0.7 eV. The tendency of opening the gap is found to be strongest in the actually observed AFM-$[110]_2$ structure below the Néel temperature. The widely varying transport data in the literature are critically examined. They indicate a gap smaller than 0.1 eV, consistent with the present calculations, a strong influence of N-vacancy-induced doping carriers and possibly localization effects associated with the distortions accompanying the loss of antiferromagnetic ordering above the Néel temperature.

DOI: 10.1103/PhysRevB.79.035125 PACS number(s): 72.80.Ga, 71.15.Mb, 71.20.Ps

I. INTRODUCTION

The transition-metal (TM) nitrides such as the transition-metal carbides are known as refractory hard metallic compounds characterized by high hardness, excellent electrical and thermal conductivities, and good corrosion resistance.[1,2] They are extremely good for high-temperature oxidation protection coatings. Most of their technological applications in thin film or bulk form have been based on this favorable combination of properties. Recently, their electronic and magnetic properties have also received renewed attention.[3–6] VN (Ref. 7) has been found to be superconducting and recently TiN has been proposed to be a superinsulator.[8]

Among the transition-metal nitrides, CrN has a unique antiferromagnetic (AFM) configuration.[9] At room temperature, CrN is paramagnetic and has the rocksalt structure with lattice constant a_c=4.14 Å. However, upon cooling below 273–286 K, a simultaneous structural and magnetic phase transition takes place. The magnetic ordering is such that pairs of ferromagnetic (FM) planes with alternating spin directions[9–12] are aligned perpendicular to the [110] direction. This phase transition is accompanied by a (0.56–0.59)% increase in the atomic density and a distortion of the structure which becomes orthorhombic P_{mna}. It shows hysteresis of 2–3 K and the transition width is extremely sensitive to the N concentration. Corliss *et al.*[9] measured a magnetic moment of $2.36\mu_B$ per Cr atom. Another experiment by Ibberson and Cywinski[11] reported a larger value of about $3.17\mu_B$ per Cr atom.

Given the fundamental and technological interest in CrN a lot of experimental and theoretical work has been done. Although the structural properties and magnetic properties of CrN are thus well established, the same cannot be said about the electrical properties. Early results[10,13] obtained a resistivity as a function of temperature with metallic behavior. The samples used were either powders or polycrystalline films. In these studies CrN showed metallic behavior both in the paramagnetic state and in the antiferromagnetic state below 286 K, although the resistivity dropped by (30–70)% below the transition. Herle *et al.*[14] did measurements on chemically synthesized CrN powder and their resistivity measurements indicate semiconductor behavior with a band gap of 0.09 eV as measured from resistivity. Constantin *et al.*[15] measured resistivity of single-phase CrN_{1-x} with $x \leq 0.05$ thin films which were grown on a MgO (001) substrate using molecular-beam epitaxy. These films show semiconductor behavior for temperatures above 285 K with a band gap of 0.07 eV, but below 260 K metallic behavior is observed. Their data show a hysteresis of about 20 K width. On the other hand, Gall *et al.*[16] using a magnetron sputter deposition technique[17] grew crystalline thin films of CrN_{1-x} with $x \leq 0.03$ also oriented along (001) and on MgO (001) substrates and reported distinct semiconductor characteristics for a large range in temperature without any discontinuities. In fact, no structural transformation is observed in his data which all pertain to the rocksalt structure. Magnetic properties were not measured, so it is not clear if his films undergo a transition to an ordered AFM phase or not. They also measured optical absorption and concluded that there is an optical band gap of 0.7 eV. They hence suggested that CrN could be a Mott-Hubbard-type insulator in the sense that the correlation energy drives the opening of the gap.

Not only do the different groups disagree on the temperature behavior of the resistivity, but they also disagree on the order of magnitude. Remarkably, the resistivities measured by the different groups show up to 6 orders of magnitude difference among them. References 10 and 15 obtain resistivities on the order of mΩ cm at room temperature while Ref. 14 obtains kΩ cm resistivities. This large variation among experimental data suggests that this is influenced primarily by defects, in particular N concentration. In the case of powder samples the grain boundaries could also play a significant role. Among the various measurements, the ones of Gall *et al.*[16] stand out because they provide the only optical measurements of a gap and a much larger gap is deduced than in any of the previous experiments.

On the theory front Filippetti *et al.*,[18,19] using local spin-density approximation (LSDA), find that assuming cubic symmetry the lowest energy occurs for AFM ordering along [110] but with the spins changing every layer instead of every two layers. We will denote this as $[110]_1$ and note that this is equivalent to $[001]_1$ and is usually called the AFM-I ordering. If the orthorhombic distortion P_{nma} is applied, however, they find that the experimentally observed $[110]_2$ magnetic ordering becomes the ground state. They explain this in terms of a magnetic stress: bonds between antiferromagnetically coupled neighbors are under tensile stress, while bonds between ferromagnetically coupled atoms are under compressive stress. In the $[110]_2$ magnetic configurations, the stress can be relieved by an orthorhombic distortion because in the (001) plane, two of its neighbors are AFM coupled and two are FM, while in the $[110]_1$ structure, it cannot be relieved because all four nearest-neighbor Cr atoms are FM coupled. This forces the system to go from cubic to orthorhombic accompanied by a shear compression of 2% along the [110] direction. The orthorhombic to cubic structure is connected by $a=2a_c \sin(\alpha/2)$, $b=a_c \cos(\alpha/2)$, and $c=a_c$ with α slightly less than 90°. In terms of electronic structure, non-spin-polarized calculations show a high peak in the density of states (DOS) at the Fermi level. Once magnetic moments are formed, the states split and the Fermi level moves to a valley in the DOS, independently of the ordering, whether FM, AFM $[110]_1$, or $[110]_2$. However, LSDA shows definitely a metallic behavior. Because the DOS at the Fermi level is small, it could be called a weak metal.

However, it is well known from studies of TM oxides and related materials that LSDA underestimates the Coulomb effects of the narrow *d* bands and hence can erroneously predict metallic behavior in systems which actually do have a band gap. The so-called "LSDA+U" (LSDA corrected by Hubbard Coulomb terms for the *d* electrons) method has been very successful in describing systems with very strong electronic correlations. The question is if this is also the case for moderately correlated early TM nitrides, such as CrN. The LSDA+U approach, introduced by Anisimov *et al.*[20] adds the orbital-dependent Coulomb interactions to LSDA and subtracts their average behavior so as to avoid double counting. In this paper we study how the LSDA+U approach affects the electronic structure and whether it supports a Mott-insulator behavior.

The computational method, in particular the LSDA+U, aspects are described in Sec. II. An important question is of course, what values of *U* are appropriate for the nitrides. In the next section (Sec. II A) we present various estimates of *U*, including a recent approach by Cococcioni and de Gironcoli.[21] However, we take mostly an empirical approach to this question and use our estimates only as a guide to determine a reasonable range of values. We then examine how the properties behave as function of *U*. An important consideration here is that if we apply LSDA+U theory to CrN, we should also make sure to still obtain physically correct results for the neighboring TiN, VN, and MnN with similar values of *U*. In particular, it is well known that all of these are metallic and furthermore TiN and VN are not even magnetic. We next present results for FM, AFM $[110]_1$, and AFM $[110]_2$ CrN as functions of *U* in Sec. III. We also check the results for TiN, VN, and MnN. In Sec. IV we present a discussion of our results in the context of a critical examination of the available experimental data and make an attempt at clarifying the seemingly contradictory transport results. Finally, we summarize our conclusions in Sec. V.

II. COMPUTATIONAL METHOD

We use the density-functional theory (DFT) method in the local spin density approximation (LSDA) (Ref. 22) with the exchange-correlation parametrization by von Barth and Hedin[23] in the full potential (FP) linear muffin-tin orbital (LMTO) method.[24,25] The FP-LMTO method uses a highly optimized basis set consisting of muffin-tin orbitals with smoothed Hankel functions as envelope functions. The smooth interstitial quantities are calculated using a fine Fourier transform mesh and the Brillouin-zone (BZ) integration is carried out using the tetrahedron method with a well-converged *k* mesh based on the division of reciprocal unit cell in ten equal parts in each direction for structures with cubic symmetry and for the orthorhombic structure by an equivalent density.

The partially filled localized 3*d* orbitals are treated using the LSDA+U method,[20] treating the double-counting terms in the fully localized limit.[26,27] This means that LSDA is expected to produce the correct solution in the atomic limit with integer occupations $n_{m\sigma}=1$ or 0 rather than the mean-field uniform occupations $n_{m\sigma}=N_\sigma/(2l+1)$, where N_σ is the total number of electrons of a given spin. Thus, in this atomic limit the double-counting term exactly cancels the explicitly added *U* terms. This is the more plausible assumption for strongly correlated systems. The program follows the rotationally invariant formulation of Liechtenstein *et al.*,[28] which is written in terms of density matrices rather than occupation numbers in a specific basis set of localized orbitals. In a rotationally averaged approximation,[29] we have

$$E_{\mathrm{LSDA+U}} = E_{\mathrm{LSDA}} + \frac{(U-J)}{2}\sum_\sigma [\mathrm{Tr}\ \rho^\sigma - \mathrm{Tr}(\rho^\sigma \cdot \rho^\sigma)]. \quad (1)$$

Our actual implementation has a more complex interaction and double-counting term, which includes the nonspherical terms describing the *m* dependence of the Coulomb interaction,[28]

$$E^U = \frac{1}{2}\sum_{m\sigma} \langle mm''|V_{ee}|m'm''\rangle \rho^\sigma_{mm'}\rho^{-\sigma}_{m''m'''} + (\langle mm''|V_{ee}|m'm'''\rangle - \langle mm''|V_{ee}|m'''m'\rangle)\rho^\sigma_{mm'}\rho^\sigma_{m''m'''}, \quad (2)$$

$$E_{\mathrm{dc}} = \frac{1}{2}\left\{ Un(n-1) - J\sum_\sigma [n^\sigma(n^\sigma-1)]\right\}, \quad (3)$$

with $n=n^\uparrow+n^\downarrow$ and $n^\sigma=\mathrm{Tr}\ \rho^\sigma$ and $E_{\mathrm{LSDA+U}}=E_{\mathrm{LSDA}}+E_U-E_{\mathrm{dc}}$. Hence open *d*-shell configurations can be specified by the choice of the density matrix. In particular, in the present case, we can start from a density matrix which satisfies cubic symmetry and with t_{2g} orbitals filled while e_g orbitals are

empty. We note that independent of our starting point this is the density matrix we approximately converge to. The occupations of the filled states are of course not exactly equal to 1 because of hybridization, but they remain close to 1 to about 10%. The total-energy functional is then not only a functional of density but also a function of the density matrix for d electrons, and taking the derivative with respect to this density matrix leads to an additional (nonlocal) potential for d electrons. Again, in the simple spherical average approximation, this becomes

$$V^{\sigma}_{mm'} = (U-J)\left[\frac{1}{2}\delta_{mm'} - \rho^{\sigma}_{mm'}\right], \tag{4}$$

while the full expression for the nonspherical case is

$$V^{\sigma}_{mm'} = \sum_{m''m'''} \langle mm''|V_{ee}|m'm'''\rangle \rho^{-\sigma}_{m''m'''} + (\langle mm''|V_{ee}|m'm'''\rangle - \langle mm''|V_{ee}|m'''m'\rangle)\rho^{\sigma}_{m''m'''} - U\left(n-\frac{1}{2}\right) + J\left(n^{\sigma}-\frac{1}{2}\right). \tag{5}$$

We can see that it will tend to shift up unoccupied states by $(U-J)/2$ and occupied states down by $(U-J)/2$. Further shifts among different states of different m values are dictated by the nonspherical terms. The Coulomb interactions $\langle mm''|V_{ee}|m'm'''\rangle$ are expressed in terms of Clebsh-Gordon coefficients and Slater F^k integrals,

$$\langle mm''|V_{ee}|m'm'''\rangle = \sum_k a_k(mm'm''m''')F^k, \tag{6}$$

which we take from tabulated Hartree-Fock calculations[30] except for the F^0 term which is strongly screened by the environment and by definition equal to U. For the d orbitals the average exchange parameter J is expressed as $J=(F^2+F^4)/14$ and these are assumed not to be influenced by screening. We use $J=0.94$ eV. The ratio of F^4/F^2 is about 0.625 for all $3d$ elements.

The LSDA+U method is only one possible way to treat the d-band Coulomb effects. An alternative approach is the self-interaction correction (SIC) method.[31] We are not aware of any calculations for CrN or other transition-metal mononitrides using this approach. For monoxides, the two approaches were compared by Anisimov *et al.*[32] The authors cautioned in that paper that their LSDA+U had trouble reproducing the nonmagnetic character of the early monoxides whereas SIC reproduced this feature correctly. However, this was an early version of LDA+U, which is somewhat different from the presently used rotationally invariant LSDA+U version. The LSDA+U approach both has the disadvantage of including an empirical parameter U and the advantage of simplicity compared to the SIC approach.

A. Estimates of U

Essentially, U is defined by the energy difference[33]

$$U = E(d^{n+1}) + E(d^{n-1}) - 2E(d^n), \tag{7}$$

where each of the total energies refers to the energy of the localized d-electron system embedded in its environment.

TABLE I. Estimates for U. EAM1: unpolarized excited-atom model and EAM2: spin-polarized excited-atom model; the values in oxides are from Ref. 32.

	Ti	V	Cr	Mn
EAM1	2.24	2.52	2.77	3.0
EAM2	2.42	2.69	3.0	3.28
$F^0/6$	2.83	3.12	3.06	3.65
Oxides	3.5	4.0		7.8

One approach is to calculate these, using a constrained density-functional approach, in which the hopping from the local d electron to the other orbitals in the system is turned off and treating the system as a localized impurity problem.[33] Recently, an alternative linear-response formulation was proposed.[21]

First, we consider the excited-atom model.[34,35] In this model, one assumes that the screening charge is completely confined within the atomic sphere in which the d electron is added or removed. Furthermore, it is argued that it can be approximately represented by the first unoccupied orbital.[36,37] This is typically a more diffuse orbital and can thus represent the free-electron-like screening charge piling up within the atomic sphere of the site on which the d occupation is changed.

In the present case, it is the $4s$ orbital, and thus we obtain the following simple expression for U:

$$U = E(d^{n+1},s^{m-1}) + E(d^{n-1},s^{m+1}) - 2E(d^n,s^m). \tag{8}$$

m here is the number of s electrons. We start out with $n=4$ and $m=2$ and ignore that a threefold occupation of an s state violates Pauli's principle. After all, the s electron here merely represents screening charge. The total energies are free-atom total energies calculated in LSDA. A slightly different model is obtained by doing this calculation spin polarized as follows:

$$U = E(d_{\uparrow}^{(n/2)+1},d_{\downarrow}^{n/2},s^{m-1}) + E(d_{\uparrow}^{n/2},d_{\downarrow}^{n/2},s^m) - E(d_{\uparrow}^{(n/2)+1},d_{\downarrow}^{(n/2)-1},s^m) + E(d_{\uparrow}^{n/2},d_{\downarrow}^{(n/2)-1},s^{m+1}). \tag{9}$$

The results of these models for Ti, V, Cr, and Mn are given in Table I. The purely atomic values without any screening follow the same slightly increasing trend with increasing atomic number and we can see that the screened values correspond to about 1/6 of the unscreened atomic values. This indicates an approximate dielectric constant of 6, which seems reasonable compared to, e.g., the high-frequency dielectric constant of GaN.

The excited-atom model is meant to represent metallic type screening and is thus considered an upper limit for the screening or a lower limit for the U values. We note that Cococcioni obtain values for metallic Fe which are quite close between the excited-atom model and their linear-response approach.

For comparison, it is useful to consider the values in oxides reported by Anisimov *et al.*[32] Unfortunately, these authors did not consider CrO. However, it is clear that for the

other cases, the values in oxides are significantly larger than in the nitrides and a maximum value for Cr would be about 5 eV. One expects the values in oxides to be larger because oxides are more ionic and thus have less efficient screening.

Next, we consider the approach of Cococcioni and de Gironcoli.[21] These authors consider the curvature of the total energy versus occupation numbers, as opposed to consisting of a piecewise linear function, to be the origin of the error in local-density approximation (LDA), which is to be corrected by the LDA plus Hubbard U (LDA+U) approach. They also use a constrained DFT approach and consider the difference between a self-consistently calculated curvature and its noninteracting Kohn-Sham value as U. In other words,

$$U = \frac{\partial^2 E}{\partial q_l^2} - \frac{\partial^2 E^{\mathrm{KS}}}{\partial q_l^2}, \tag{10}$$

where E is the self-consistent total energy including the screening when the occupation of the local orbital at site l is changed, and E^{KS} does not include this screening but merely includes the effects of hybridization of the local orbital with the rest of the system. Subtracting this term is thus equivalent to switching off the hopping terms between the local orbital and the rest of the system in the approach of Ref. 33. It is obtained by noting that the sum in one-electron eigenvalues (noninteracting Kohn-Sham energy) corresponds to the energy of the first iteration when shifting the potential of the d orbital on the lth site. This is essentially the Andersen force theorem. In fact, instead of changing the occupation numbers and calculating the corresponding potential shift required to constrain the occupation to the desired one, they switch, by means of a Legendre transformation, to treating the potential shifts as the independently varied parameter. Thus, their prescription for U becomes

$$U = \frac{\partial \alpha_l^{\mathrm{KS}}}{\partial q_l} - \frac{\partial \alpha_l}{\partial q_l} = (\chi^{\mathrm{KS}})_{ll}^{-1} - \chi_{ll}^{-1}, \tag{11}$$

where $\chi_{ll'} = \partial q_l / \partial \alpha_{l'}$ is a linear-response function. In practice the latter is calculated numerically for a supercell in which a shift $\alpha_{l'}$ is included on site l'. One simply evaluates the corresponding induced charge on the other d-sites l once self-consistently and once after the first iteration. One then needs to invert the χ matrices and look for the on-site element. We calculate the on-site and Cr-Cr nearest neighbor χ_{ij} in an eight-atom conventional cell. Assuming the more distant neighbor χ_{ij} is zero, we then set up the χ_{ij} matrix for a larger $2\times2\times2$ cell; i.e., we calculate the Fourier transform $\chi_{ij}(\mathbf{q}) = \Sigma_{\mathbf{T}} \chi_{i,j+\mathbf{T}}$ for $\mathbf{q}=0$, i.e., the long-range response matrix and invert this matrix to obtain $[\chi(\mathbf{q}=0)]_{ii}^{-1}$, i.e., the on-site element of the inverse matrix. These are the quantities entering the definition of U in Eq. (11). For CrN, we find a value of $U=3.7$ eV, which is somewhat larger than that obtained within the excited-atom model.

Finally, however, we should remember that all these simple rotationally averaged estimates give us the value of $U_{\mathrm{eff}} = U - J$ rather than the actual U value in our nonspherical LSDA+U implementation. Given the value of $J=0.94$ eV, a reasonable range for U in CrN is between about 3.0 and 5.0 eV. The Cococcioni approach would suggest 4.6 eV and the excited-atom approach 3.7 eV.

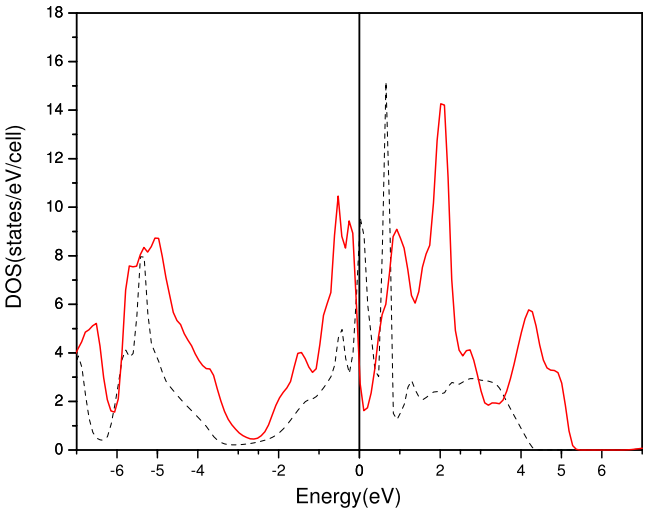

FIG. 1. (Color online) The density of states for spin-polarized cubic (black) and distorted AFM $[110]_2$ structure (red).

III. RESULTS

A. LSDA results

We first need to make sure that our LMTO calculations reproduce the earlier results with LSDA. For cubic rocksalt structure the nonpolarized calculations show a high partially filled peak at the Fermi energy. The spin-polarized calculations lower the total energy per CrN pair of atoms by 0.17 eV relative to the nonpolarized calculations. Hence the system is magnetic. Cr has a magnetic moment of about $2\mu_B$ per atom. A magnetic moment of $2\mu_B$ might be interpreted as Cr being divalent with a d^4 configuration. The threefold-degenerated majority-spin state $t_{2g}^{\uparrow}$ would then be completely filled while the minority $t_{2g}^{\downarrow}$ would have one electron in it and the e_g states of both spins would remain empty because they are pushed up much higher by the crystal field or covalent interactions with N. In reality, our calculations give as occupations for the various orbitals: $t_{2g\uparrow}$, 2.16, $t_{2g\downarrow}$, 0.73, $e_{g\uparrow}$ 0.96 and, $e_{g\downarrow}$ 0.4. Thus, clearly, the e_g orbitals are not empty and the total charge per Cr is 4.25, meaning that the valency is less than 2. This is consistent with the band structures which indicate a strong hybridization of the Cr d and N p bands, showing that we are far from the ionic level and have strong covalentlike bonding.

In agreement with Filippetti *et al.*[18] we also find that the observed experimental orthorhombic structure with AFM ordering along the $[110]_2$ is the ground state. Also in agreement with their results, we find that the density of states is reduced near the Fermi energy compared to the spin-polarized calculations leading to a dip in the density of states or a weak metal as seen in Fig. 1. Furthermore, the DOS at the Fermi level is lower in the $[110]_2$ configuration than in the ferromagnetic configuration by about 10 eV per cell per spin.

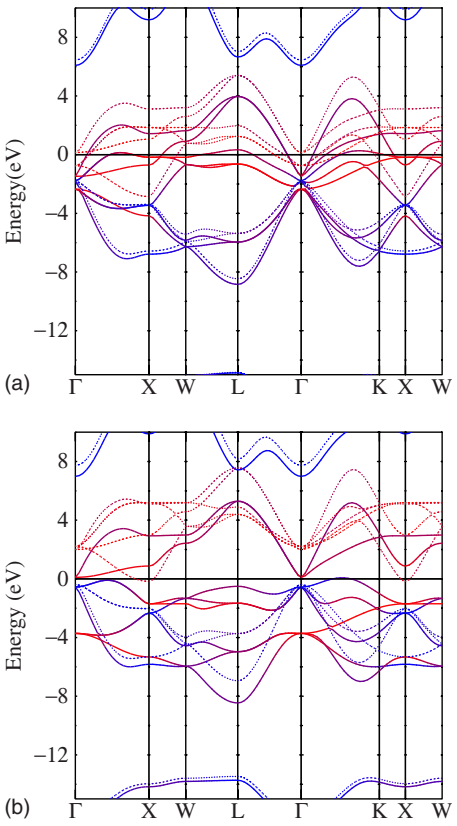

FIG. 2. (Color online) Band structure of FM CrN in (a) LSDA and (b) LSDA+U with $U=5$ eV. Solid lines: majority spin and dotted lines: minority spin. The bands are colored with a mix of red and blue with red in proportion to their d weight and blue corresponding to all other orbitals.

B. LSDA+U for FM CrN

To build insight we first consider the "Hubbard-U" effects on the FM cubic case. We calculated the band structure and magnetic moments for various values of U.

Figure 2 shows the band structure of FM CrN in both LSDA and LSDA+U with a value of $U=5$ eV. This is an upper limit on the value of U according to our estimates in Sec. II. The degree of hybridization of Cr d orbitals with other orbitals is indicated by coloring the bands with a mixture of blue and red with the weight factor of red indicating the d partial weight at each k point. The reader of the printed black and white version is referred to the electronic online version to view this information which cannot conveniently be provided in any other way. The majority spin is indicated by solid line and the minority spin by dotted line. One can see from the purple color that in LSDA, there is a large amount of hybridization at many k points. Interestingly, the lowest threefold-degenerate band at Γ is the d-$t_{2g\uparrow}$ band (as indicated by its red color) but the lower bands away from Γ are predominantly N-2p-like as indicated by their bluish color. The next eigenvalues at Γ are blue and thus not d-like. They are the up- and down-spin t_{1u} N p states which are very close together. Some of the spin-up bands connected to it change color abruptly and become predominantly d-like as we move away from Γ. The doubly degenerate states at Γ are the d-e_g-like bands. We can see that the minority-spin (down) e_g lies above the Fermi level while the majority spin lies below it. We can think of the bands connecting to these states at Γ as predominantly e_g-like. The minority spin $t_{2g\downarrow}$ also lies below the Fermi level. The N $2p$ orbitals form strong σ bonds with the Cr e_g orbitals because they point directly toward each other. Hence the bands derived from them show up as bluish purple and the corresponding d-like bands show up as reddish purple at most k points. An exception occurs at Γ where they cannot interact by symmetry. This explains the abrupt changes in the orbital character of the bands near Γ mentioned above. Some of the mainly t_{2g}-orbital-derived bands show up as almost completely d-like (pure red) along a large portion of the Brillouin zone, indicating their weak interaction with N.

When U is switched on, the occupied d bands are down shifted, while the empty d bands shift up. In particular, we may notice the large shift of the occupied majority-spin t_{2g} bands, originating from the d-like threefold-degenerate state at Γ. A gap opens between a N $2p$-like valence-band maximum (VBM) and majority-spin e_g bands at Γ. The Fermi level shifts significantly relative to the bands as can be seen, for example, by the fact that now we see the top of the N s-like bands in the bottom of the energy window, i.e., about 15 eV below the Fermi level. The t_{2g} minority-spin bands are also shifted up and one of these bands forms the conduction-band minimum at X. The conduction-band minimum at Γ on the other hand is an e_g majority-spin-like band. The valence-band maximum occurs along $\Gamma-K$ and the indirect gap between them is just zero for this value of U. The smallest direct gap is slightly below 1 eV and one expects a strong direct transition between parallel bands near Γ along $\Delta=\Gamma-X$

This situation is sometimes called a "charge-transfer" insulator.[38] The difference between a charge-transfer insulator and a true Mott insulator is that the gap driven by Coulomb interactions occurs not strictly between d states but between anion p states and metal d states.

It is of interest that if we consider Cr to be nominally trivalent in the nitride, $t_{2g\uparrow}$ is then fully occupied and $t_{2g\downarrow}$ is fully empty once a gap is opened. The actual density matrix we obtain is close to this. Clearly, adding a large U brings us closer to the ionic limit. It also raises the question if the opening of a gap in CrN is specifically related to the possibility of integer occupation of the $t_{2g\uparrow}$ states. However, we emphasize that this is a somewhat oversimplified picture.

As far as the magnetic moments are concerned, even with a small value of $U=1$ eV the magnetic moment on Cr atom increases significantly. This is because the on-site Coulomb repulsion reduces the p-d hybridization thus increasing the magnetic moment on Cr. The magnetic moment on Cr atom varies from $2.6\mu_B$ for $U=1$ eV to $3\mu_B$ for $U=5$ eV.

C. LSDA+U for AFM CrN

Here, we consider the effect of LSDA+U on different magnetic configurations. We now use a lower limit of 3 eV for the value of U. We have already seen that FM CrN still is metallic in this case. Here we consider distorted AFM $[110]_2$

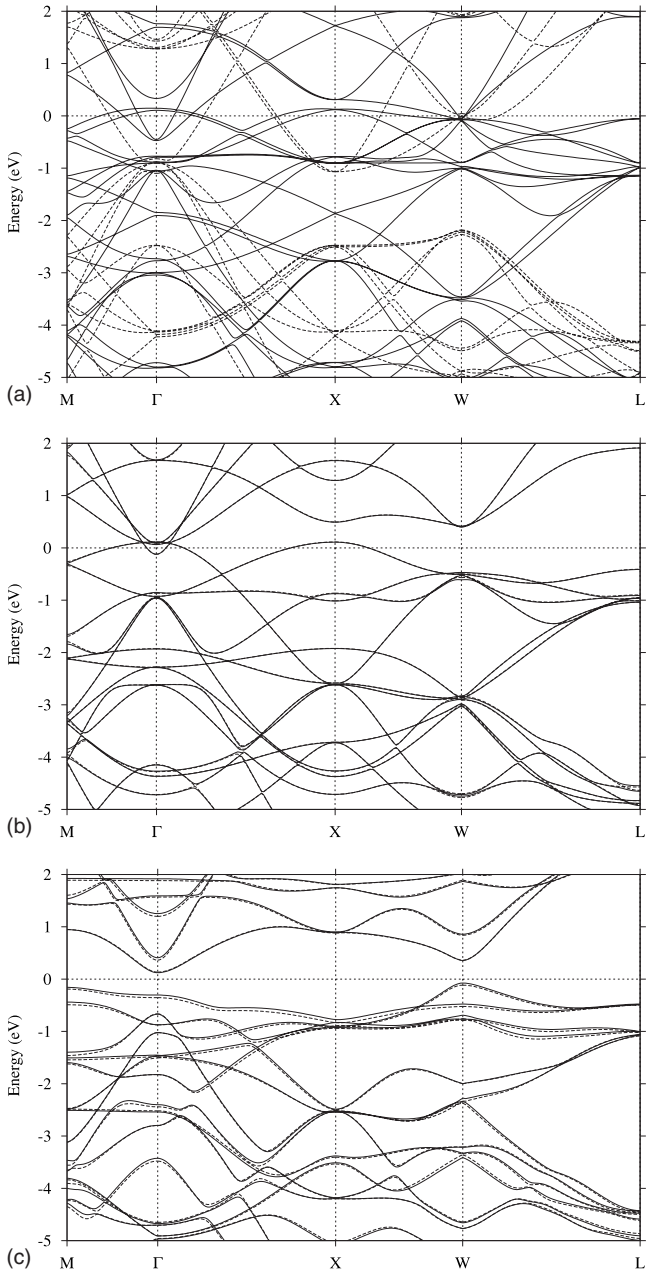

FIG. 3. Band structure of (a) FM (solid line: majority and dashed line: minority spin), (b) AFM-$[110]_1$, and (c) AFM-$[110]_2$ CrN with $U=3$ eV and $J=0.941$ eV all shown in the BZ of AFM $[1100]_2$.

and cubic AFM $[110]_1$. The bands for these two cases along with that of FM CrN are shown in Fig. 3 in the BZ relevant for the $[110]_2$ unit cell for the sake of comparison. The k points shown correspond to $M=\pi/a,0,0$, $X=0,\pi/b,0$, $W=\pi/a,3\pi/2b,0$, and $L=0,\pi/b,\pi/c$, with the x axis along the cubic [110] direction in which the spins are ordered and y perpendicular to it. In other words, the x and y axes are rotated 45° from the cubic axes. Since the unit cell consists of four layers in this direction, the bands along $\Gamma-X$ are essentially those of the fcc $\Sigma=\Gamma-K-X$ direction folded in two and the bands along $\Gamma-M$ are the same bands folded in four, hence the numerous degeneracies seen at M (and X in

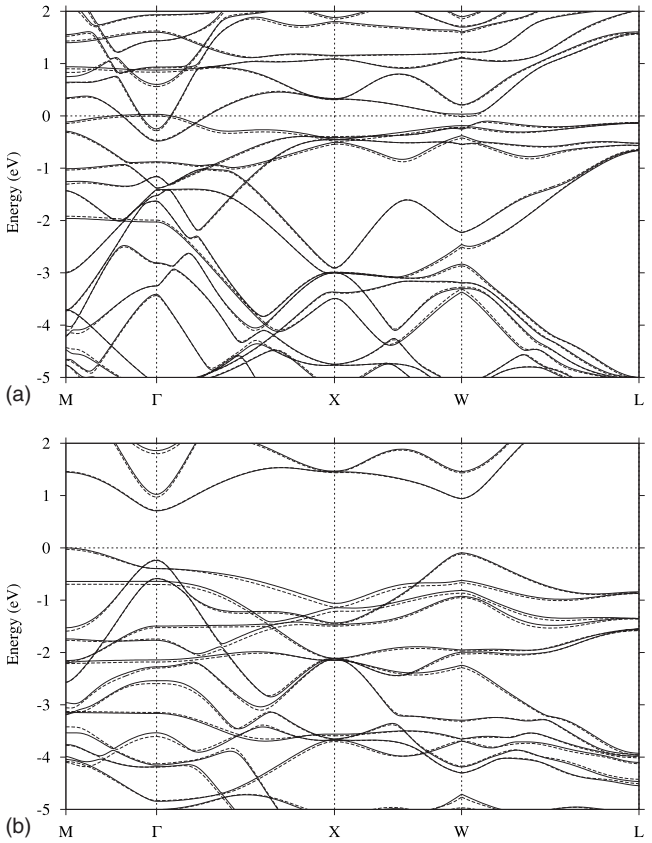

FIG. 4. Band structure of AFM-$[110]_2$ CrN with $J=0.941$ eV. (a) $U=1$ eV and (b) $U=5$ eV

the FM case). When we consider the AFM-$[110]_1$ order, the fcc unit cell is doubled since it consists of two layers, and the bands still stay degenerate at M but some of the degeneracies we had at X are already lifted. When we consider AFM $[110]_2$ the bands at M also split.

With this overall understanding of the folding of the bands in mind, we can now see that the band structure stays metallic in FM and AFM $[110]_1$ but a gap opens in AFM $[110]_2$. The band gap in the latter case is about 0.4 eV for $U=3$ eV. This gap already starts opening at $U\approx 2.5$ eV. Apparently, the AFM-$[001]_2$ configuration, which even in LSDA suppresses the density of states near E_F, helps to open the gap.

In Fig. 4 we give further information on how the bands evolve with the value of U for the AFM-$[110]_2$ case. Starting from a small value of $U=1$ eV, we find that the first two bands below E_F at Γ move up gradually as we increase U [the case for $U=3$ eV is shown in Fig. 3(c)] while the first band above E_F moves down and becomes the highest valence band. Thus, again, U splits certain bands apart but the behavior is somewhat more complex than in the FM case. The net effect is that bands are removed from the region near E_F and a gap opens up. The gap is still indirect. When the gap first opens at $U=2.5$ eV, the VBM is at W, but eventually for $U=4$ eV it moves to M and can become as large as 0.7 eV. On the other hand, for the AFM $[110]_1$ case, the gap only just starts to open at $U\approx 4$ eV and is indirect. A direct gap of slightly less than 1 eV exists near the Γ point.

Unfortunately, we cannot presently study the paramagnetic state in which presumably magnetic moments are still present but point in random directions. However, it appears that among the three magnetic configurations studied, the gap is smallest in the FM alignment and largest for the actual AFM-$[110]_2$ configuration for any given value of U.

Viewing the density of states for all three cases, in Fig. 5 we may note a remarkable resemblance. Although only in the AFM-$[110]_2$ case a true gap opens, the DOS is quite small at E_F even in the other cases. In conclusion, in all cases, CrN appears to be at the brink of becoming a charge-transfer insulator, even for fairly small values of U of about 2–3 eV.

D. LSDA+U band structure of TiN, VN, and MnN

Here, we return to the question of the nearby transition-metal nitrides. Among these, neither TiN nor VN show magnetic ordering. VN is known to become superconducting at low temperature[7] and TiN was recently shown to behave as a superinsulator.[8] MnN is known to be an antiferromagnet.[6] If we use similar values of U as suggested in Sec. III A, do we still obtain reasonable results for TiN, VN, and MnN? Their band structures for a value of $U=5$ eV are shown in Figs. 6–8.

As can be seen for VN, the band structure starts to show a spin splitting for $U=5$ eV, in disagreement with experiment. It still is metallic in agreement with experiment. For the somewhat smaller value of $U=3$ eV, both TiN and VN stay nonmagnetic and metallic, although some shifts in the bands take place from the LSDA band structure. Also for MnN, we can clearly see that the band structure stays metallic even for U as large as 7 eV. In this case, the ground state is AFM $[001]_1$ but for simplicity we here consider the FM state. In conclusion, values near 3 eV or lower for TM nitrides yield results in good agreement with the basic facts for TiN, VN, and MnN but values of 5 eV or larger start giving some unphysical results.

IV. DISCUSSION

At first sight, the experimental results appear difficult to reconcile with the data. Although we can obtain a gap as large as 0.7 eV with a reasonable U value of 4 eV, it occurs only for the AFM-$[110]_2$ case, which would occur below T_N. On the other hand, the only measurement of a gap as large as 0.7 eV occurs for paramagnetic CrN.[16] Perhaps, even more puzzling, Constantin *et al.*[15] obtain semiconductor behavior above T_N but metallic behavior below T_N, which is seemingly exactly opposite to our results.

We thus need to examine not only our results but also the experiments critically. First of all, the optical-absorption data show a strong increase in absorption at 0.7 eV but the absorption does not go to zero below 0.7 eV. The absorption coefficient is still almost on the order of 10^4 cm^{-1} almost down to zero. This is fairly large for an indirect-gap transition. However, there is no sign of intraband free-carrier absorption. On the other hand, the resistivity data of Gall *et al.*[16] can according to their paper be described by $\rho = \rho_0 \exp(\sqrt{T_0/T})$ with $\rho_0 = 0.665 \times 10^{-2}$ Ω cm and T_0

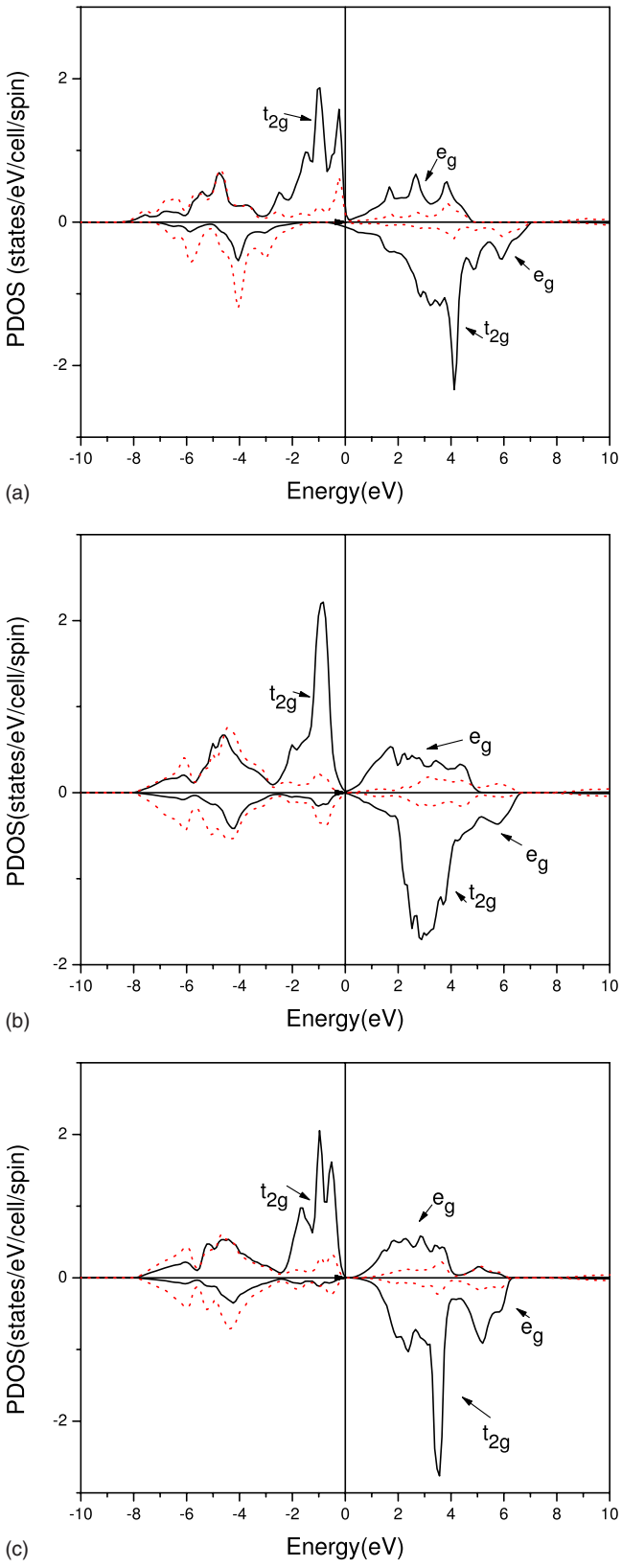

FIG. 5. (Color online) Partial densities of states for (a) FM, (b) AFM $[110]_1$, and (c) AFM $[110]_2$ with $U=3$ eV and $J=0.941$ eV. For the AFM cases, the DOS is shown for one of the atoms; the other atom has of course spin-up and -down reversed. Black solid lines: Cr d and red dashed lines: N p.

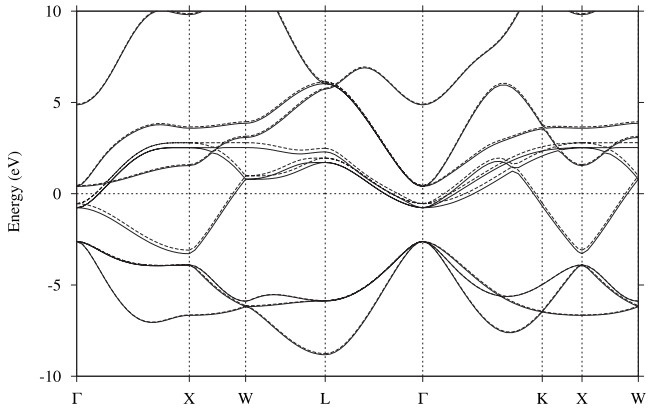

FIG. 6. Band structure in LDA+U for rocksalt TiN; $U=5$ eV and $J=0.898$ eV.

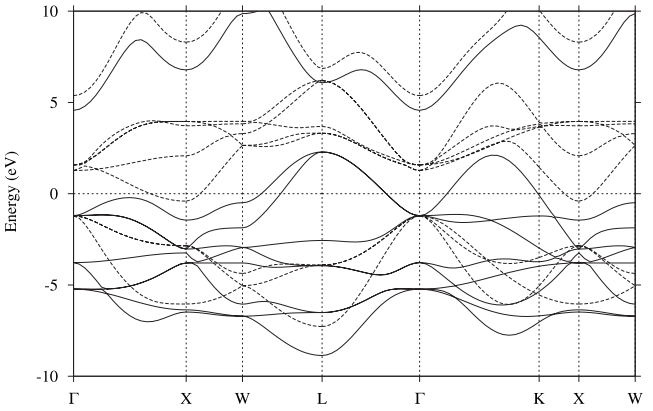

FIG. 8. Band structure in LDA+U for rocksalt MnN; $U=5$ eV and $J=1.160$ eV.

$=1800$ K. The temperature behavior is indicative of hoppinglike conduction between localized states. If we replot the same data in a $\ln \rho$ versus $1/T$ plot (Fig. 9), we can indeed see that the data do not follow a straight line as would be expected for a normal semiconductor, where the slope would indicate $E_g/2k$. It is also clear however that the slopes are small and indicate a gap of at most 20–40 meV. This is compatible with the gap deduced by Constantin *et al.*[15] in the region above T_N and also by Herle *et al.*[14] Thus the data indicate an almost vanishing gap with a very low concentration of carriers which furthermore appear to become localized and a strong optical transition or large joint density of states at about 0.7 eV.

This is consistent with our calculated band structure for FM CrN at $U \approx 5$ eV or AFM $[110]_2$ at $U \approx 3$ eV or AFM $[110]_1$ at $U \approx 4$ eV. Indeed, in all these cases, which we take to be as guide for the behavior in the disordered paramagnetic state, we find a strongly depleted density of states near the Fermi level with essentially a zero or very small indirect band gap and a set of nearly parallel bands just below and above the Fermi level, separated by slightly less than 1 eV, suggesting that this may be the origin of the 0.7 eV strong increase in optical absorption. Unfortunately, we cannot directly deal with the paramagnetic disordered state for which the optical absorption was measured. At this point, however, we have no experimental indications that the optical absorption shows strong changes with magnetic order.

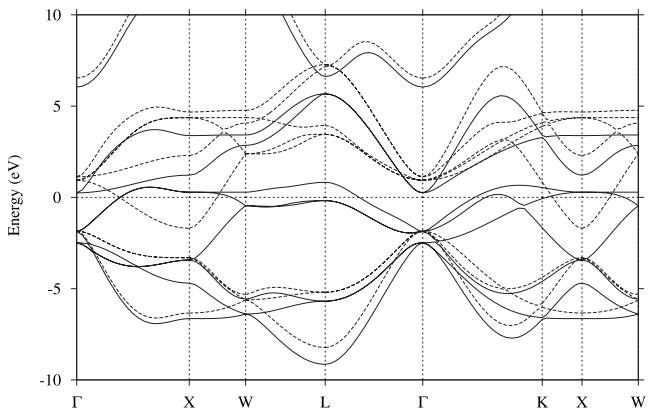

FIG. 7. Band structure in LDA+U for rocksalt VN; $U=5$ eV and $J=0.991$ eV.

Returning now to the puzzling data of Constantin *et al.*,[15] we first note that the magnitude of their resistivities on the order of mΩ cm is similar to the one of Browne *et al.*[10] and both studies show an increase in resistivity upon going above T_N. The only difference is that the latter obtain metallic temperature behavior above T_N while the former obtain semiconductinglike temperature behavior. This is indicative of a disorder-induced localization. It is well known that localization in doped semiconductors depends critically on the carrier density. Above a critical density, the system becomes metallic, while below that density the electrons stay trapped in local perturbations.[39] In the present case, it is likely that the carriers arise from N vacancies which would act as donors. The main differences between different samples appear to come from different N concentrations. It is interesting that the magnetic disorder in the paramagnetic state would seem to result in effective potential fluctuations which can trap electrons. It should be recalled that the magnetic transition in this case is accompanied by a structural transformation.

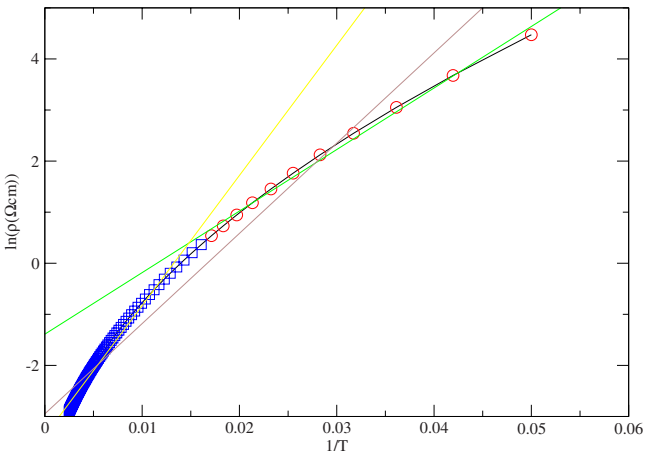

FIG. 9. (Color online) Plot of resistivity data of Gall *et al.*(Ref. 16) as $\ln \rho$ versus $1/T$. The various straight lines indicate linear fits to the data (indicated by circles) at low or high T or the full range. Their slopes provide upper and lower limits of the effective transport gap E_g.

Thus, it seems conceivable that as the magnetic order is breaking apart in small local regions, local structural distortions take place and help to localize the carriers. Because the temperature range measured by Constantin *et al.*[15] above T_N is fairly small, it is difficult to ascertain whether the resistivity in this regime is better described by a thermally activated $\ln \rho \propto T^{-1}$ or $\ln \rho \propto T^{-1/2}$ hopping behavior, although the latter would be more compatible with the present viewpoint. The fact that a jump in resistivity occurs at T_N indicates that a strong increase in the strength of the disorder potential occurs at this point. From this point of view, it might appear that in samples of Gall *et al.*,[16] the disorder is strong enough to be in the localization regime down to 20 K. Whatever the origin of this disorder, this might also be responsible for the suppression of the magnetic ordering in their samples and hence the absence of any structural transition.

It is clear that to make further progress on this problem, a key issue is to suppress the N vacancies in CrN so as to expose the true nature of the intrinsic CrN electronic structure without the doping issue. Optical-absorption measurements as function of temperature in samples which do exhibit the magnetic and structural transitions in conjunction with direct calculation of the optical spectra from our band structures would be very useful.

V. CONCLUSIONS

Our LSDA+U calculations provide support for the idea that CrN may be close to a charge-transfer insulator transition. With reasonable values of U in the range of 3–5 eV, we find that the density of states near the Fermi level is strongly depleted by the spin separation of the states. In the case of the AFM-$[110]_2$ configuration a small gap actually opens even for U as small as 3 eV. Furthermore a smallest direct gap slightly less than 1 eV can be seen in these band structures and could be responsible for the onset of strong optical absorption observed to occur at 0.7 eV. Interestingly, we find that in the actually observed AFM-$[110]_2$ structure below the Néel temperature, the tendency of opening the gap is the strongest.

It is clear that CrN is a fairly weakly correlated material, but nonetheless Hubbard-U-type effects deplete the density of states near the Fermi level by separating spin-up and spin-down Cr d states. However, the gap is between anion p states and metal d states and thus better described as a charge-transfer insulator than a Mott insulator.[38] From a critical examination of the experimental data, it also appears that CrN is at best a nearly zero gap semiconductor with a gap $E_g \ll 0.1$ eV. Nitrogen vacancies play a significant role in doping the material and may lead effectively to a metalliclike conduction below T_N even if the real material has a gap at these temperatures because the high concentration of carriers and the overlap of the defect impurity band with the conduction band lead to a degenerate Fermi-gas limit. The occurrence of semiconductorlike behavior above T_N in one set of data was tentatively attributed to localization when the carrier density is low enough and may be related to random fluctuations related to the onset of disorder which is accompanied by a structural distortion. Values of U larger that 4 eV could lead to an even larger gap but would be inconsistent with results for nearby TM nitrides which need to remain metallic and nonmagnetic.

ACKNOWLEDGMENTS

This work was supported by the Office of Naval Research under Grant No. N00014-02-1-0880 and the National Science Foundation under Grant No. DMR-0710485. The computations were done at the Ohio Supercomputing Center.

*Present address: National Renewable Energy Laboratory, Golden, CO 80401, USA.

[1] U. Wiklund, M. Bromark, M. Larsson, P. Hedenqvist, and S. Hogmark, Surf. Coat. Technol. **91**, 57 (1997).
[2] C. Nouveau, M. A. Djouadi, O. Banakh, R. Sanjinés, and F. Lévy, Thin Solid Films **398–399**, 490 (2001).
[3] M. S. Miao, Pavel Lukashev, Aditi Herwadkar, and W. R. L. Lambrecht, Phys. Status Solidi C **2**, 2516 (2005).
[4] M. S. Miao and W. R. L. Lambrecht, Phys. Rev. B **71**, 214405 (2005).
[5] W. R. L. Lambrecht, M. S. Miao, and Pavel Lukashev, J. Appl. Phys **97**, 10D306 (2005).
[6] W. R. L. Lambrecht, Margarita Prikhodko, and M. S. Miao, Phys. Rev. B **68**, 174411 (2003).
[7] B. R. Zhao, L. Chen, H. L. Luo, M. D. Jack, and D. P. Mullin, Phys. Rev. B **29**, 6198 (1984).
[8] V. M. Vinokur, T. I. Baturina, M. V. Fistul, A. Yu. Mironov, M. R. Baklanov and C. Strunk, Nature (London) **452**, 613 (2008).
[9] L. M. Corliss, N. Elliott, and J. M. Hastings, Phys. Rev. **117**, 929 (1960).
[10] J. D. Browne, P. R. Liddell, R. Street, and T. Mills, Phys. Status Solidi A **1**, 715 (1970).
[11] R. M. Ibberson and R. Cywinski, Physica B **180-181**, 329 (1992).
[12] M. N. Eddine, F. Sayetat, and E. F. Bertaut, C. R. Seances Acad. Sci., Ser. B **269**, 574 (1969).
[13] Y. Tsuchiya, K. Kosuge, Y. Ikeda, T. Shigematsu, S. Yamaguchi, and N. Nakayama, Mater. Trans., JIM **37**, 121 (1996).
[14] P. S. Herle, M. S. Hedge, N. Y. Vasathacharya, S. Philip, M. V. R. Rao, and T. Sripathi, J. Solid State Chem. **134**, 120 (1997).
[15] C. Constantin, M. B. Haider, D. Ingram, and A. R. Smith, Appl. Phys. Lett. **85**, 6371 (2004).
[16] D. Gall, C. S. Shin, R. T. Haasch, I. Petrov, and J. E. Greene, J. Appl. Phys. **91**, 5882 (2002).
[17] D. Gall, C. S. Shin, R. T. Spila, M. Odén, M. J. H. Senna, J. E. Greene, and I. Petrov, J. Appl. Phys. **91**, 3589 (2002).
[18] A. Filippetti, W. E. Pickett, and B. M. Klein, Phys. Rev. B **59**, 7043 (1999).
[19] A. Filippetti and N. A. Hill, Phys. Rev. Lett. **85**, 5166 (2000).
[20] V. I. Anisimov, F. Aryasetiawan, and A. I. Lichtenstein, J. Phys.: Condens. Matter **9**, 767 (1997).
[21] M. Cococcioni and S. de Gironcoli, Phys. Rev. B **71**, 035105

(2005).
[22] P. Hohenberg and W. Kohn, Phys. Rev. **136**, B864 (1964); W. Kohn and L. J. Sham, *ibid.* **140**, A1133 (1965).
[23] J. W. Tucker, J. Phys. C **5**, 2064 (1972).
[24] O. K. Andersen, Phys. Rev. B **12**, 3060 (1975); O. K. Andersen, O. Jepsen, and M. Sob, in *Electronic Band Structure and its Applications*, edited by M. Yussouff (Springer, Heidelberg, 1987), p. 1.
[25] M. Methfessel, M. van Schilfgaarde, and R. A. Casali, in *Electronic Structure and Physical Properties of Solids: The Uses of the LMTO Method*, edited by H. Dreyssé, Lecture Notes in Physics Vol. 535 (Springer-Verlag, Berlin, 2000), pp. 114-471.
[26] M. T. Czyżyk and G. A. Sawatzky, Phys. Rev. B **49**, 14211 (1994).
[27] A. G. Petukhov, I. I. Mazin, L. Chioncel, and A. I. Lichtenstein, Phys. Rev. B **67**, 153106 (2003).
[28] A. I. Liechtenstein, V. I. Anisimov, and J. Zaanen, Phys. Rev. B **52**, R5467 (1995).
[29] S. L. Dudarev, G. A. Botton, S. Y. Savrasov, C. J. Humphreys, and A. P. Sutton, Phys. Rev. B **57**, 1505 (1998).
[30] Joseph B. Mann, Los Alamos Internal Report No. LA-3690 UC 34, Physics, TID-4500, 1967 (unpublished).
[31] A. Svane and O. Gunnarsson, Phys. Rev. Lett. **65**, 1148 (1990).
[32] V. I. Anisimov, J. Zaanen, and O. K. Andersen, Phys. Rev. B **44**, 943 (1991).
[33] V. I. Anisimov and O. Gunnarsson, Phys. Rev. B **43**, 7570 (1991).
[34] J. F. Herbst, R. E. Watson, and J. W. Wilkins, Phys. Rev. B **17**, 3089 (1978).
[35] W. Lambrecht, N. J. Castellani, and D. B. Leroy, Solid State Commun. **56**, 1073 (1985).
[36] W. R. L. Lambrecht, Phys. Rev. B **62**, 13538 (2000).
[37] D. A. Papaconstantopoulos, W. E. Pickett, B. M. Klein, and L. L. Boyer, Phys. Rev. B **31**, 752 (1985).
[38] J. Zaanen and G. A. Sawatzky, Can. J. Phys. **65**, 1262 (1987).
[39] P. P. Edwards, T. V. Ramakrishan, and C. N. R. Rao, J. Phys. Chem. **99**, 5228 (1995).